Research Square

Preprints are preliminary reports that have not undergone peer review.
They should not be considered conclusive, used to inform clinical practice,
or referenced by the media as validated information.

Improving mechanical properties and thermal stability of halogen-free flame retardants using di(hydroxyethyl methacrylate) phosphate and spacers

A. K. Al-Hamzawi
ali.alhamzawi@qu.edu.iq
University of Al-Qadisiyah
Zahraa M. Gafil
University of Al-Qadisiyah
Hind Shabbani
University of Al-Qadisiyah
B. A. Buravov
Volgograd State Technical University
O. O. Tuzhikov
Volgograd State Technical University
O. I. Tuzhikov
Volgograd State Technical University

Research Article

Keywords: Halogen-free flame retardants, phosphate-containing methacrylates, synthesis, spacers, thermal stability, mechanical properties

Posted Date: May 18th, 2026

DOI: https://doi.org/10.21203/rs.3.rs-9614421/v1

License: This work is licensed under a Creative Commons Attribution 4.0 International License.
Read Full License

Additional Declarations: No competing interests reported.

Version of Record: A version of this preprint was published at Journal of Inorganic and Organometallic Polymers and Materials on August 3rd, 2026. See the published version at https://doi.org/10.1007/s10904-026-04467-7.

Improving mechanical properties and thermal stability of halogen-free flame retardants using di(hydroxyethyl methacrylate) phosphate and spacers

A. K. Al-Hamzawi[a*], Zahraa M. Gafil[a], Hind Shabbani[a], B. A. Buravov[b], O. O. Tuzhikov[b], O. I. Tuzhikov[b]

a University of Al-Qadisiyah, 58002, Al-Diwaniyah City, Iraq

b Volgograd State Technical University, 400005, Volgograd, Russia,

*e-mail: ali.alhamzawi@qu.edu.iq

Abstract

Three halogen-free phosphate-containing oligoester methacrylates (HFPOEMs) were synthesized, including a monomer without spacers (HFPOEM-1) and spacers incorporating either flexible aliphatic linkages (HFPOEM-2) or rigid aromatic linkages (HFPOEM-3). Structural analyses (FTIR and NMR) confirmed the successful incorporation of phosphate groups and spacer units, while DSC results revealed a processing behavior dependent on the type of spacer, with reactivity decreasing as steric constraints increased.

Thermogravimetric analysis showed a significant improvement in thermal stability upon incorporation of the spacer, with the aromatic spacer system exhibiting the highest thermal resistance (T_5% = 279 °C) and char yield (44.3 wt%), attributed to enhanced structural rigidity and carbonization. Physical-Mechanical testing highlighted a distinct structure–property relationship, where the flexible aliphatic spacer markedly improved both tensile strength (49.9 MPa) and elongation at break (7.8%), indicating improved toughness through increased segmental mobility and stress dissipation. Conversely, the aromatic spacer improved strength while limiting ductility due to restricted chain mobility. The results of the Limited Oxygen Index (LOI) show that the samples containing spacers have slightly lower LOI values

compared to the sample without spacers, following the order: HFPOEM-1 (LOI = 31.6) > HFPOEM-2 (LOI = 30.5) > HFPOEM-3 (LOI = 29.7).

KEYWORDS: *Halogen-free flame retardants; phosphate-containing methacrylates; synthesis; spacers; thermal stability; mechanical properties.*

1. Introduction

Polymeric materials are present everywhere in modern society; however, their inherent flammability and rapid combustion pose significant safety concerns. Consequently, the challenge is to ensure that these materials remain both useful and safe. Polymer flame retardancy can be achieved either by physically blending flame retardants into the polymer matrix, known as additive flame retardants, or by chemically incorporating them during synthesis, referred to as reactive flame retardants.

Halogen-based flame retardants exhibit high flame-retardant efficiency and were extensively utilized throughout the past century. However, Halogenated flame-retardants release toxic dioxins and corrosive gases during combustion, which are harmful to human and animal health [1]. Halogenated flame retardants are biologically accumulative and cause severe ecological damage. Consequently, many countries and regions have restricted their use. The European Union, for example, has prohibited several halogen-containing substances in electrical and electronic equipment, including pentabromodiphenyl ether, polybrominated biphenyl, polybromodiphenyl ether, and octabromodiphenyl ether. For these reasons, halogenated flame retardants are now seldom investigated in the flame-retardant field due to their limited future potential [2].

Therefore, halogenated and toxic flame retardants have been progressively replaced by low- or non-toxic alternative flame retardants, including organic phosphorus, nitrogen, and phosphorus-nitrogen-based flame retardants. These types are commonly known as halogen-free flame retardants and are generally classified

into two categories: additive halogen-free flame retardants, which are physically blended with polymers, and reactive halogen-free flame retardants, which are chemically incorporated into polymer chains before or during polymerization process. Various additive halogen-free systems have been developed, such as mineral compounds, antimony compounds, and red phosphorus. However, These systems often require high loadings to achieve effective flame retardancy, which may adversely affect the other properties of polymeric materials, particularly their mechanical properties [1, 3-5].

Currently, the majority of studies have focused on organophosphorus flame retardants (OP-FRs) due to their effective fire-retardant performance and, more importantly, their superior environmental sustainability [5-13]. Examples of OP-FRs include tri(acryloyloxyethyl) phosphate (TAEP), triphenyl phosphate (TPP), dimethyl methylphosphonate (DMMP), tributyl tetradecyl phosphonium chloride (TTPC), and bisphenol A diphenyl phosphate (BADP). These compounds predominantly act in the condensed phase by generating phosphoric acid and polymetaphosphoric acid, thereby promoting char formation in the burning zone of polymeric materials. Moreover, phosphorus-derived radical species, including $HPO_2^{\bullet}$, $PO^{\bullet}$, $PO_2^{\bullet}$ and $HPO^{\bullet}$, can also volatilize into the gas phase, where they effectively scavenge $H^{\bullet}$ and $OH^{\bullet}$ radicals, thereby inhibiting oxidation reactions. Many studies have further demonstrated that, at equivalent molar concentrations, some phosphorus-based flame retardants in the gas phase exhibits higher flame-retardant efficiency than halogen components [3, 14-21].

It is well established that oligoester acrylates (OEAs) are widely used as polymerizable oligomers with applications in construction, transportation, aerospace, adhesives, coatings, and electronics. However, their high flammability, low thermal stability, and poor physical-mechanical properties limit their use in certain applications. One common strategy to improve the flame-retardant properties of OEA polymers involves reacting epoxide acrylates or hydroxyethyl acrylates with

phosphoric acid or phosphorus acid chlorides containing two or three reactive chloro groups leads to the formation of di- and tri-esters [6 -13, 22]. Nevertheless, the relatively poor mechanical properties of phosphorus-based halogen-free esters make it difficult to simultaneously achieve high flame retardancy and satisfactory mechanical performance in oligoesters, which remains a key challenge for both academic research and industrial applications.

Recently, an important strategy for improving the mechanical properties of polymeric materials has involved the synthesis of functional monomers using reactive compounds containing hydrocarbon chains of different lengths and various structural spacers between the reactive centers of the functional end groups [23-28]. Consequently, considerable efforts in our previous studies [3, 29 - 32] have been devoted to improving the flame-retardant, thermal, and mechanical properties of oligoester methacrylates (OEMs). In this regard, a series of phosphate-containing oligoester methacrylates (FOEMs) and phosphine-containing oligoester methacrylates (PPCs) were successfully synthesized by reacting phosphorus oxychloride or phosphorus trichloride with glycidyl methacrylate, as well as different structures of aliphatic diepoxide oligomer (E-181) and aromatic diepoxide oligomer (ED-20), which can be incorporated into oligoester chains as spacers connecting two phosphate groups or two phosphine groups.

The results of these studies [6, 33-34] showed that the impact strength of photocured phosphine-containing polymers with an aliphatic spacer (PPC-2) and an aromatic spacer (PPC-3) increased by 3 and 2.5 times, respectively, compared with the corresponding polymer PPC-1 (without spacer). The incorporation of E-181 (aliphatic spacer) into the structure of PPC-2 polymer raised the temperature at 5% mass loss (T5%) by 7°C, whereas ED-20 (aromatic spacer) increased the temperature at 5% mass loss (T5%) by 49°C. This was accompanied by an increase in the char residue yield at 400 °C from 29 wt% to 34 wt% and 44 wt%, respectively. The limiting oxygen index (LOI) results indicate that the spacer-free polymer (PPC-1)

exhibits the highest LOI value (≈28%), whereas the introduction of spacers slightly reduces the LOI to approximately 27% for the aromatic spacer (PPC-3) and to about 24% for the aliphatic spacer (PPC-2). For the phosphate-containing oligoester methacrylates (FOEMs), the impact strength of the thermal-cured polymer containing an aliphatic spacer (FOEM-2) reached 11.0 kJ/m², while that of the polymer containing an aromatic spacer (FOEM-3) reached 4.5 kJ/m², which are 5 and 2 times, respectively, higher than the values of the reference polymer FOEM-1 (without a spacer). The use of the synthesized compounds as binders enabled the preparation of fiberglass-reinforced plastics with a limiting oxygen index (LOI) of approximately 40 vol%. The smoke generation values during pyrolysis for the fiberglass-reinforced plastics FOEM-1, FOEM-2, and FOEM-3 were 75, 58, and 85 m²/kg, respectively. Furthermore, the heat release values of the investigated phosphate-containing oligoester methacrylates were 1.5–2 times lower than those of fiberglass-reinforced plastics prepared using the diepoxide oligomer ED-20 as a binder.

To meet the requirements for high flame retardancy and environmental safety, a phosphate-based flame-retardant monomer, tri(acryloyloxyethyl) phosphate (TAEP), was synthesized by reacting phosphorus oxychloride ($POCl_3$) with 2-hydroxyethyl acrylate (HEA). Then, the obtained product was mixed with pentaerythritol tetrathioglycolic (PETTG) at different mass ratios in the presence of benzoyl peroxide as a radical initiator, and the resulting mixtures were thermally cured to produce halogen-free, phosphorus–sulfur-containing flame retardants [13]. The results revealed that increasing the sulfur content accompanied by a decrease in phosphorus content led to a gradual reduction in the LOI value from 31.5% to 26.2% for the cured resins, whereas the refractive index was enhanced with increasing sulfur content. It has been reported that a phosphate-based, trifunctional monomer, tris(4-hydroxybutyl acrylate) phosphate, has been prepared by reaction of $POCl_3$ with 4-hydroxybutyl acrylate, and subsequently cured under UV irradiation in the presence of Darocur 4265 as a photoinitiator [10]. The UV-cured polymer exhibited good

flame retardancy, with a LOI value of up to 31%, and maintained thermal stability up to 235 °C.

Based on the above studies, the present work reports the synthesis of novel phosphate-containing halogen-free oligoester methacrylates (HFPOEMs) incorporating spacer linkages with either aliphatic or aromatic structures to enhance the thermal stability and mechanical performance of the resulting materials. The chemical composition and molecular structures of the synthesized HFPOEMs were confirmed by FT-IR and NMR spectroscopy. The curing processes of HFPOEMs were investigated by differential scanning calorimetry (DSC). The flame-retardant performance of the peroxide-cured HFPOEMs was evaluated using the limiting oxygen index (LOI) test, while their thermal degradation behavior and mechanical properties were systematically investigated by thermogravimetric analysis (TGA) and standard mechanical testing methods.

2. Experimental part

2.1. Materials

Phosphorus oxychloride ($POCl_3$, purity: 99%, CAS No. 10025-87-3), supplied from Sigma-Aldrich, was purified by distillation before use. 2-Hydroxyethyl methacrylate (HEMA, purity: 97%, CAS No. 868-77-9), triethylamine (TEA, purity: 99.5%), ethyl ether ($(CH_3CH_2)_2O$, purity: ≥99%, CAS No. 60-29-7), tripropylene glycol (TPG, purity: 97%, CAS No. 24800-44-0) and Bisphenol A ethoxylate (BAEO-6, CAS No. 32492-61-8, Mn = ~492 g/mol, EO/phenol = 3) were purchased from Merck (Germany), and used as received. All other materials and solvents were obtained from commercial sources and used as received, without additional purification.

2.2. Synthesis and reactions

2.2.1. Tris [2-(methacryloyloxy) ethyl] phosphate (HFPOEM-1)

Tris [2-(methacryloyloxy) ethyl] phosphate (HFPOEM-1) was synthesized through the phosphorylation of 2-hydroxyethyl methacrylate (HEMA) using $POCl_3$ as

previously described [8,12,13]. A mixture of 38.28 g HEMA (0.294 mol) and 34.46 g TEA (0.341 mol) was dissolved in 100 mL of ethyl ether into a 250 mL four-neck reactor equipped with a thermometer, a calcium chloride drying tube and an electrical agitator. Subsequently, with constant stirring, a solution of 15 g $POCl_3$ (0.098 mol) and 20 mL ethyl ether was slowly added dropwise into the reactor (under nitrogen flow) at 0 °C using an ice-bath. Then the reaction mixture was kept under stirring around 12 h at room temperature. The resulting triethylamine hydrochloride salt was removed by filtration, and the filtrate was twice extracted by aqueous solutions of HCl (1 M), $NaHCO_3$ (10%), and saturated NaCl. The resulting product was dried over anhydrous sodium sulfate, and the solvent was evaporated under reduced pressure. The product obtained was colorless transparent liquid, well soluble in acetone. The FT-IR, ^{1}H, ^{13}C and ^{31}P NMR spectra of HFPOEM-1 are presented as follows.

FT-IR (cm^{-1}): C-H (2963 cm^{-1}), C=O (1721 cm^{-1}), C=C (1648 cm^{-1}), P=O (1264 cm^{-1}), R-O-R (1186 cm^{-1}), and P-O-C (985 cm^{-1}).

^{1}H NMR NMR spectrum (300 MHz, $CDCl_3$) δ, ppm: C=C$\underline{H_2}$ (5.99 _ 5.90 and 5.44_5.38), OP–O–C$\underline{H_2}$ (5.01_4.98), C$\underline{H_2}$–O–C(O) (4.31 _ 4.13), $\underline{H_3}$C–C (1.77).

^{13}C NMR spectrum (75 MHz, $CDCl_3$) δ (ppm): O–$\underline{C}$(O) (166.99 _ 164.97), $\underline{C}$=CH_2 (136.25 _ 134.51), C=$\underline{C}H_2$ (127.97 _ 125.23), PO–O–$\underline{C}H_2$ (71.79), (CO)O–C$\underline{H_2}$ (64.89), $\underline{C}H_{3group}$ (17.62).

^{31}P NMR spectrum (121 MHz, $CDCl_3$) δ, ppm: -2.2 ppm for $O=P(OR)_3$.

2.2.2. (((((propane-1,2-diylbis (oxy)) bis(propane-2,1-diyl)) bis (oxy)) bis (oxo-phosphan etriyl)) tetrakis (oxy)) tetrakis (ethane-2,1-diyl) tetrakis (2-methyl acrylate) (**HFPOEM-2**)

HFPOEM-2, containing aliphatic spacer, was synthesized through a two-step esterification. In the first step, in a 250 mL four-necked reactor equipped with a thermometer, an electrical agitator, a calcium chloride drying tube, a dropping funnel and a reflux condenser, preliminarily purged with dry nitrogen for 30 min, a solution

of 100 mL of ethyl ether, 25.52 g of HEMA (0.196 mol) and 22.97 g of TEA (0.227 mol) was successively loaded. Then, with constant stirring, a mixture of 15 g of $POCl_3$ (0.098 mol) and 20 mL of ethyl ether was slowly added dropwise into the reactor at 0 °C under nitrogen flow. After the mixture was added, the resulting intermediate was continuously stirred for 3 h at ambient temperature under N_2 protection. In the second step, ethyl ether (30 mL), tripropylene glycol (TPG, 9.41 g, 0.049 mol), and triethylamine (TEA, 11.9 g, 0.118 mol) were mixed and placed in the dropping funnel. The mixture was then added dropwise to the reactor at a controlled rate to ensure that the reaction temperature did not exceed 5 °C. Then, the resulting mass was stirred at ambient temperature for 12 h with continuous stirring and N_2 purging. The precipitated triethylamine hydrochloride salt was separated by filtration, and the resulting filtrate was subsequently washed twice with aqueous solutions of HCl (1 M), $NaHCO_3$ (10%), and saturated NaCl. The obtaining product was then dried over anhydrous sodium sulfate, and the solvent was removed under reduced pressure. The final product was obtained as a colorless, transparent liquid exhibiting good solubility in acetone. The corresponding FTIR, ^{31}P, ^{1}H and ^{13}C NMR spectral data of product HFPOEM-2 are summarized as follows.

FT-IR (cm^{-1}): C-H (2961 cm^{-1}), C=O (1721 cm^{-1}), C=C (1636 cm^{-1}), P=O (1266 cm^{-1}), R-O-R (1186 cm^{-1}), and P-O-C (98 cm^{-1}).

^{1}H NMR NMR spectrum (300 MHz, $CDCl_3$) δ, ppm: C=C$\underline{H}_2$ (5.86 and 5.63), OP–O–C$\underline{H}$ (4.56), C(=O)–O–C$\underline{H}_2$ (4.44 _ 4.40), OP–O–C$\underline{H}_2$ (4.25 _ 4.14), CH_2–O–C$\underline{H}$< (3.68 _ 3.59), C$\underline{H}_2$–O– CH< (3.49 _ 3.43), C$\underline{H}_3$–C (1.95), C$\underline{H}_3$–CH (1.39 and 1.18).

^{13}C NMR spectrum (75 MHz, CDCl3) δ, ppm: O–$\underline{C}$(O) (166.80), $\underline{C}$=CH2 (135.74), C=$\underline{C}$H2 (125.83), −$\underline{C}$H(CH_3)−O−CH_2 (77.03_76.69), −$\underline{C}H_2$−O−CH< (73.98_73.72), OP–O–$\underline{C}H_2$ (72.58_71.86), OP–O–$\underline{C}$H (71.09), $\underline{C}H_2$– O–C(=O) (64.99 _ 64.78), $\underline{C}H_{3group}$ (19.12 _ 17.41).

^{31}P NMR spectrum (121 MHz, $CDCl_3$, 85% H_3PO_4) δ, ppm: (−3.18) ppm ($(RO)_2O=P–O–\mathbf{R_1}–O–P=O(OR)_2$), where $\mathbf{R_1}$ is the fragment formed as a result of incorporating the aliphatic spacer.

2.2.3. ((((((propane-2,2-diyl bis (4,1-phenylene)) bis(oxy)) bis (ethane-2,1-diyl)) bis (oxy)) bis (oxo-phosphanetriyl)) tetrakis (oxy)) tetrakis (ethane-2,1-diyl) tetrakis (2-methyl acrylate) (**HFPOEM-3**)

HFPOEM-3 (containing aromatic spacer) was synthesized via a two-step procedure. In the first step, a 250 mL four-necked round-bottom reactor equipped with a thermometer, a mechanical stirrer, a calcium chloride drying tube, a dropping funnel, and a reflux condenser was purged with dry nitrogen for 30 min. Subsequently, a solution consisting of ethyl ether (100 mL), 2-hydroxyethyl methacrylate (HEMA, 26.52 g, 0.196 mol), and triethylamine (TEA, 22.97 g, 0.227 mol) was sequentially introduced into the reactor. Subsequently, under continuous stirring, a solution of $POCl_3$ (15 g, 0.098 mol) in ethyl ether (30 mL) was added dropwise to the reactor at 0 °C under a flow. After completion of the addition, the reaction mixture was maintained under stirring for 3 h at ambient temperature under inert nitrogen atmosphere. In the second step, ethyl ether (30 mL), bisphenol A ethoxylate (BAEO-6, 24.12 g, 0.049 mol), and triethylamine (TEA, 11.88 g, 0.118 mol) were mixed and transferred to the dropping funnel. This mixture was then added dropwise to the reactor at a controlled rate while maintaining the reaction temperature below 5 °C. Subsequently, the resulting reaction mixture was further stirred at ambient temperature for 12 h under continuous nitrogen atmosphere. The precipitated triethylamine hydrochloride salt was removed by filtration, and the filtrate was successively washed with aqueous HCl (1 M), $NaHCO_3$ (10%), and saturated NaCl solution, each twice. The obtaining product was then dried over anhydrous sodium sulfate, and the solvent was removed under reduced pressure. The final product was obtained as a colorless, transparent liquid with good solubility in acetone. The

structural characterization of HFPOEM-3 was confirmed by FT-IR, ^{1}H NMR, ^{13}C NMR, and ^{31}P NMR spectroscopy, as shown below.

FT-IR (cm^{-1}): C-H (2963 cm^{-1}), C=O (1719 cm^{-1}), C=C (1636 cm^{-1}), P=O (1273 cm^{-1}), R-O-R (1192 cm^{-1}), P-O-C (987 cm^{-1}), and the aromatic group C=C stretch (1508 cm^{-1}).

^{1}H NMR NMR spectrum (300 MHz, $CDCl_3$) δ, ppm: –CH=C<u>H</u>– (7.14), –C<u>H</u>=CH– (6.83), >C=C<u>H_2</u> (5.84 and 5.61), C(=O)–O–C<u>H_2</u> (4.41), OP–O–C<u>H_2</u> (4.24), and <u>C</u>H_{3group} (1.93 and1.59).

^{13}C NMR spectrum (75 MHz, CDCl3) δ, ppm: O–<u>C</u>=O (174.27), =<u>C</u>< (165.74, 149.56 and 141.55), =<u>C</u>H– (133.42 and 119.69), >C=<u>C</u>H_2 (131.09), (CO)O–<u>C</u>H_2 (68.89), OP–O–<u>C</u>H_2 (66.93), >C< (42.98), and <u>C</u>H_{3group} (31.05 and 18.02)

^{31}P NMR spectrum (121 MHz, CDCl3, 85% H_3PO_4) δ, ppm: (−2.83) ppm ($(RO)_2O$=P–O–**R_2**–O–P=O$(OR)_2$), where **R_2** is the fragment resulting from the introduction of aromatic spacer.

2.3. Characterization and measurements

FTIR spectrometry analysis was performed using spectrophotometer (FT-IR 8400S, Shimadzu, Japan) in the range of 400 to 4000 cm^{-1}. The Infrared spectra data obtained from each measurement was then combined and realized using the Spectragryph software version 1.2. ^{31}P, ^{13}C, and ^{1}H NMR spectra of the synthesized HFPOEMs were recorded on a AV-400 (400 MHz) spectrometer, using deuteron chloroform ($CDCl_3$) as the solvent at room temperature, with the chemical shifts presented in δ (ppm). Polymerization kinetics of HFPOEM samples were studied by a differential scanning calorimeter (DSC) with a TA Model DSC 2910 (TA Instruments, Wilmington, DE, USA) under the protection of nitrogen (flow rate of 50 mL/min) and at a heating rate of 10°C/min.

Thermogravimetric analysis (TGA) measurements were carried out under a nitrogen atmosphere using a thermogravimetric analyzer STA2500 (Netzsch,

Germany). About 5 mg of each polymeric samples was placed in an aluminum crucible and heated from room temperature to 800 °C at a constant heating rate of 10 °C/min, while nitrogen was continuously purged at a flow rate of 50 mL/min. Limiting oxygen index (LOI) values for polymeric specimens were measured by a Limiting Oxygen Index Meter (NETZSCH TAURUS Instruments AG, Germany) in the range from 0 to 100% oxygen, with a measurement error of no more than 0.2% and sample dimensions of 130 × 10 × 5 mm^3, following ISO 4589-2. The physical and mechanical characteristics of cured HFPOEMs like ultimate tensile strength, elastic modulus, and elongation at break were achieved with an Instron machine (model 3366, Instron, USA) according to ASTM D-790. Three specimens were tested For each cured material with dimensions of 100 mm × 10 mm × 4 mm and the average value was determined. The impact strength tests of the cured polymers were conducted using Impact Tester (Taiwan, China) according to ASTM D256. All reported results represent the mean values of five samples.

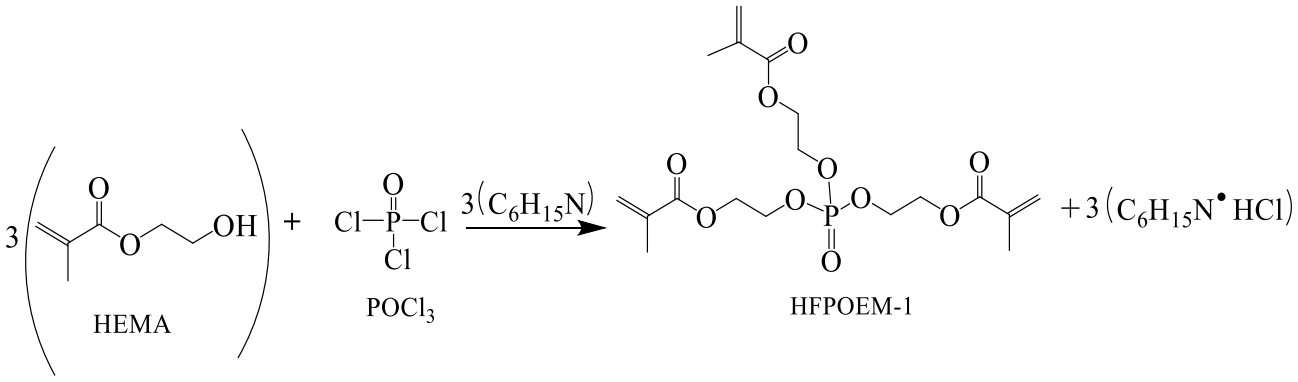
2.4. Preparation of cured samples of HFPOEMs

The free-radical polymerization of the methacrylate functional groups was initiated using benzoyl peroxide (BPO) as a thermal initiator. In a typical procedure, 0.2 g of BPO was homogeneously mixed into 40 g of each HFPOEM sample (0.5%) within a three-necked flask equipped with a mechanical stirrer and a thermometer. The mixtures were heated under constant agitation until complete dissolution of the initiator was achieved. Subsequently, the resulting solutions were poured into molds and left in an oven at 60°C for 1 h, followed by 80 °C for 1 h. After that, the materials were heated to 90°C, 100°C, 110°C, and 130°C, respectively, and maintained at each stage for 2 hours until the samples are fully cured. Finally, the resultant thermosets were allowed to cool naturally to room temperature to minimize internal residual stresses.

3. Results and discussion

3.1. Confirmation of synthesized structures of HFPOEMs

Three novel types of halogen-free phosphate-containing oligoester methacrylates (HFPOEMs) were synthesized to improve thermal stability and physical-mechanical performance of the oligoester acrylates. The chemical structures of these compounds include one without a spacer having trifunctional groups (HFPOEM-1), and two others containing either an aliphatic spacer (HFPOEM-2) or an aromatic spacer (HFPOEM-3), each possessing tetrafunctional groups. HFPOEM-1 was successfully synthesized via a one-step reaction between phosphorus oxychloride ($POCl_3$) and 2-Hydroxyethyl methacrylate (HEMA) at a 1:3 molar ratio in the presence of triethylamine (TEA) to neutralize the generated hydrochloric acid as ammonium salt. The reaction was initially maintained at 0 °C, followed by keeping the reaction mixture for 12 h at room temperature. The synthetic route for HFPOEM-

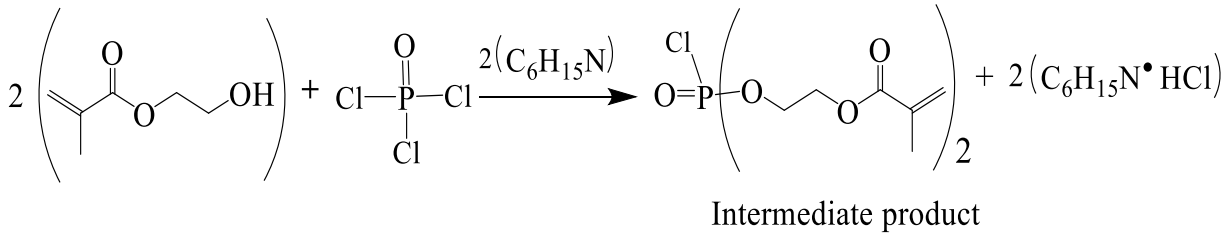


Scheme 1. Synthetic route of tris[2-(methacryloyloxy) ethyl] phosphate (HFPOEM-1)

1 is illustrated in below Scheme 1.

The preparation of halogen-free phosphate-based oligoester methacrylates containing either aliphatic or aromatic spacers was carried out via a two-step process. In the first step, the intermediate product [O=PCl(HEMA)$_2$] was synthesized by partial substitution of chlorine atoms on the phosphorus center. $POCl_3$ was reacted with

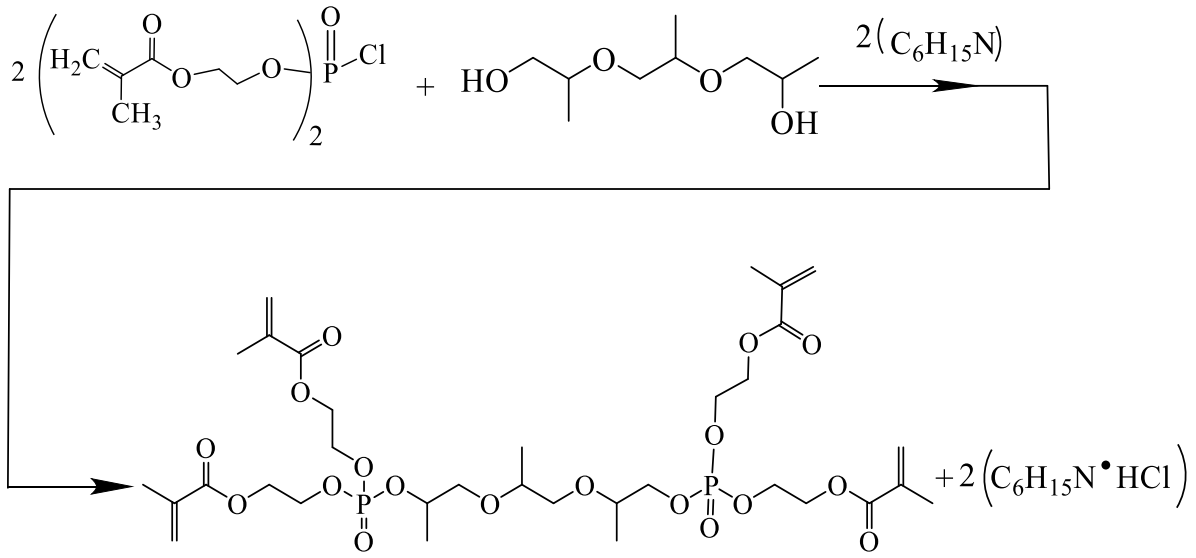
HEMA in a 1:2 molar ratio (Scheme 2) at 0 °C under a nitrogen flow. The reaction mixture was then stirred for 3 h at room temperature under N_2. In our previous study, as well as other studies [3, 7, 35-37], have confirmed that the nucleophilic substitution reaction of the first and second P–Cl bonds of POCl3 with an epoxy group or a phenolic group proceeds more rapidly than that of the third bond. This is attributed to the decrease in electrophilicity at the phosphorus center after each substitution step, as well as to steric hindrance effects. As a result, the selective reaction of HEMA with $POCl_3$ led to the formation of the intermediate product [O=PCl(HEMA)$_2$], which is formed through the selective substitution of the first two chlorine atoms of $POCl_3$ by HEMA.



Scheme 2. Synthesis of the intermediate product [O=PCl(HEMA)2]

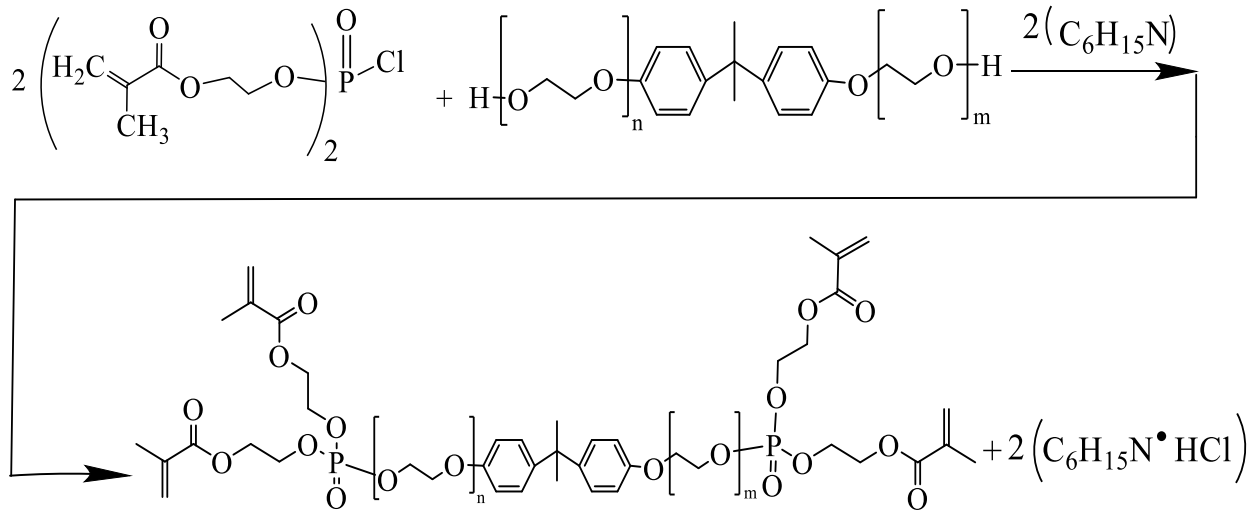
In the second step, the final HFPOEM products with spacers were synthesized by reacting the intermediate obtained from the first step with dihydroxyl compounds containing either aliphatic or aromatic moieties. Specifically, the aliphatic dihydroxyl component (TPG) was used to synthesize HFPOEM-2, whereas the aromatic dihydroxyl component (BAEO-6) was employed to synthesize HFPOEM-3. The incorporation of these spacers introduced spatial separation between the two phosphate groups within the molecular structure. The reaction began with the dropwise addition of a mixture of diethyl ether and TPG, or BAEO-6, to the intermediate, under constant stirring at a rate such that the temperature of the reaction mixture did not exceed 10 °C.

The reaction between the intermediate and the dihydroxyl component (TPG) is illustrated in the following scheme.



Scheme 3. Synthetic route of HFPOEM-2 by reaction of intermediate with TP

The second step in the synthesis of HFPOEM-3 followed the same protocol used for HFPOEM-2 and involved the reaction of the intermediate prepared in the first step with the dihydroxyl compound BAEO-6, as shown in Scheme 4.



Scheme 4. Synthetic route of HFPOEM-3 by reaction of intermediate with BAEO-6

The chemical structures of the synthesized HFPOEMs were confirmed by FT-IR spectroscopy; the corresponding spectra are presented in Figure 1. The FT-IR spectrum of HFPOEM-1 shows the complete disappearance of the hydroxyl (O–H) stretching band typically observed in the region 3600–3200 cm^{-1}, providing initial evidence for the successful synthetic reaction of HFPOEM-1. The presence of an absorption band at 1264 cm^{-1} is assigned to the P=O (phosphoryl group) stretching vibration, while the intense peaks at 985 cm^{-1} correspond to the P–O–C phosphoester bond. The retention of the vinylic (C=C) stretching at 1648 cm^{-1} and the ester carbonyl C=O at 1721 cm^{-1} indicates that the methacrylate functionality remains intact and available for subsequent polymerization. Finally, the peaks at 2963 cm^{-1} and 1186 cm^{-1} corresponded to C–H and R–O–R stretching of the HFPOEM-1 structure units, respectively.

In the FT-IR spectra of HFPOEM-2 (Figur 1), the introduction of a flexible spacer (PPG) between two phosphate groups containing methacrylate functional structures does not result in a significant difference in the spectra of HFPOEM-2 and HFPOEM-1. Importantly, similar to HFPOEM-1, the FT-IR spectrum of HFPOEM-2 shows the complete disappearance of the hydroxyl (O–H) stretching band in the region 3600–3200 cm^{-1}, indicating the completion of the chemical reaction. Additionally, an increase in the intensity of the aliphatic C–H stretching near 2970 cm^{-1} is observed, consistent with the additional methyl groups of the PPG backbone.

The IR spectrum of HFPOEM-3 provides clear evidence for the incorporation of a rigid bisphenol A ethoxylate (BAEO-6). Similar to the previous products, the complete disappearance of the hydroxyl (O–H) stretching band confirms the effective consumption of hydroxyl groups during the phosphorylation process. The spectrum exhibits the characteristic phosphate absorption band corresponding to P=O stretching at 1273 cm^{-1} and the absorption band corresponding to P-O-C 987 cm^{-1}. Notably, additional bands associated with the aromatic BAEO-6 fragment are observed, Sharp absorptions at 1608 and 1508 cm^{-1} are assigned to the C=C stretching vibrations of the

phenyl rings. Furthermore, the peaks at 1192 cm^{-1}, 1719 cm^{-1}, and 2963 cm_{-1} corresponded to R-O-R, C=O and C-H stretching of the HFPOEM-3 structure units, respectively. Importantly, the persistence of the methacrylate vinyl stretching band at 1636 cm^{-1}.

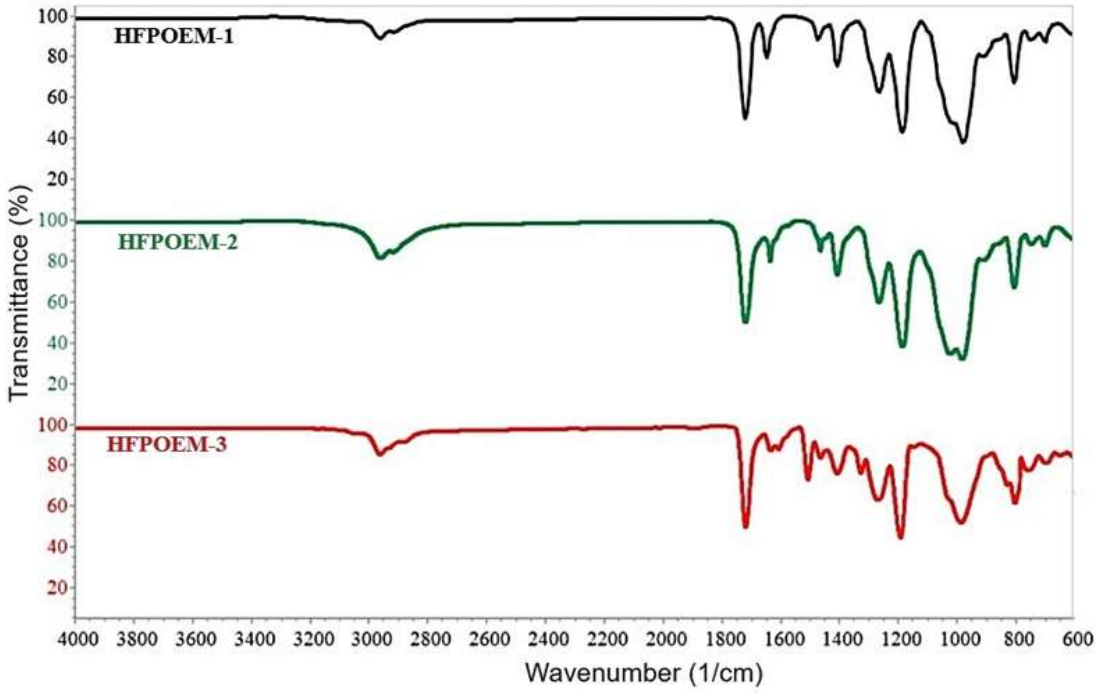


Figure 1. IR spectrum of products HFPOEM-1, HFPOEM-2 and HFPOEM-3

Furthermore, The structures and purity of HFPOEMs were characterized and confirmed by ^{1}H NMR, ^{13}C NMR and ^{31}P NMR spectroscopy. ^{1}H NMR spectrum of HFPOEM-1 monomer (Figure 2-a) shows the multiplet peaks at (5.99–5.90) ppm and 5.44–5.38) ppm, corresponding to vinyl proton resonances of methacrylate groups C=C$\underline{H}_2$, confirming the preservation of polymerizable functionalities. The resonance signals observed between 4.31–4.13 belong to C$\underline{H}_2$–O–C(O) protons, while the OP–O–C$\underline{H}_2$ protons resonate between 5.01–4.98 ppm due to the electron-with drawing effect of the phosphate ester groups. The methyl group of methacrylate $\underline{H}_3$C–C are observed as singlet peak at 1.77 ppm.

The ^{13}CNMR spectrum also corroborates the chemical structure of HFPOEM-1 (Figure 2-b), showing ester carbonyl carbons (O–$\underline{C}$(O)) in the range of 166.99 –

164.97 ppm, vinyl carbons at δ 136.25–134.51 ppm for $\underline{C}=CH_2$ and at δ 127.97–125.23 for $C=\underline{C}H_2$. The resonance observed around 71.79 ppm is assigned to the methylene carbon of the ester moieties OP–O–$\underline{C}H_2$, mean= the peak aroud 64.89 ppm is attributed to the methylene carbon within the (CO)–O–$\underline{C}H_2$ fragments. Additionally, the singlet at 17.62 ppm is assigned to the methyl group of methylmethacrylate.

The ^{31}P NMR spectrum (Figure 2-c) exhibits a single sharp resonance at δ= -2.2 ppm, which is characteristic of phosphate triesters. These data conclusively demonstrate the successful synthesis of a fully functionalized, phosphate-centered trimethacrylate monomer, characterized by high structural purity with the polymerizable functionalities remaining entirely intact.

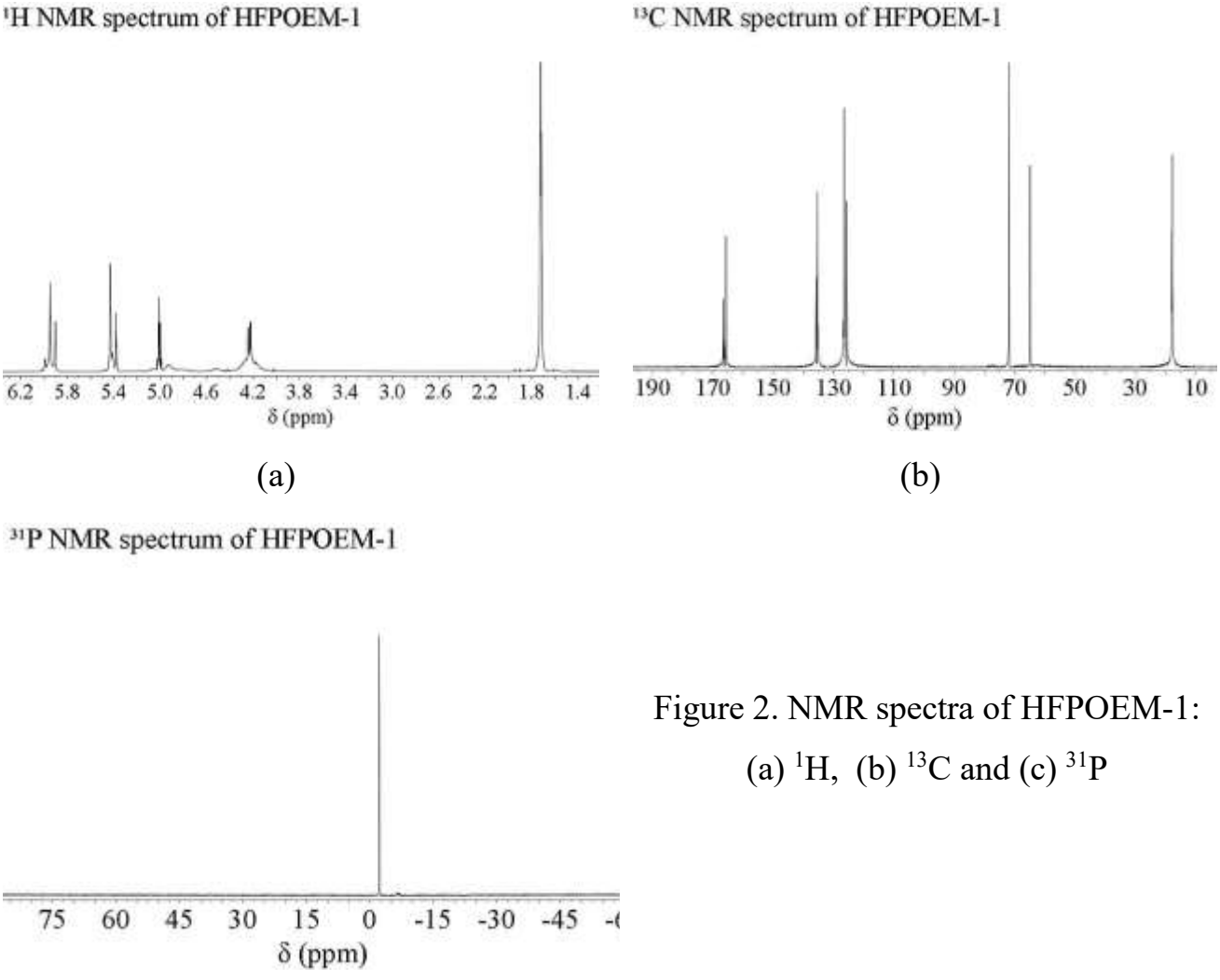


Figure 2. NMR spectra of HFPOEM-1: (a) ^{1}H, (b) ^{13}C and (c) ^{31}P

(c)

The ^{1}H NMR spectrum of HFPOEM-2 with the assignment is shown in Figure 3-a. The two groups of characteristic peaks at 5.86–5.63 ppm are obviously observed in the spectrum, which prove the existence vinyl proton of acrylate group (C=C$\underline{H}_2$) in HFPOEM-2 molecular structure. The proton of phosphate ester moiety in aliphatic spacer OP–O–C$\underline{H}$ appear as singlet at 4.56 ppm, whereas the OP–O–CH_2 protons resonate in the region 4.25–4.14 ppm. The methyl group of aliphatic spacer protons C$\underline{H}_3$–CH< is observed in the region 1.39–1.18 ppm, and the methyl group of methacrylate C$\underline{H}_3$–C appear as singlet at 1.95 ppm. Moreover, the multiplet resonance at 4.44–4.40 ppm is assigned to the methylene protons of the methacrylate group (C(=O)–O–C$\underline{H}_2$), while the two sets of multiplets appearing at 3.68–3.59 ppm and 3.49–3.43 ppm correspond to the methine (CH_2–O– C$\underline{H}$<) and methylene (C$\underline{H}_2$–O– CH<) protons, respectively, within the aliphatic spacer.

The ^{13}C NMR spectrum of HFPOEM-2 (Figure 3-b) shows ester carbonyl carbons (O–$\underline{C}$(O)) at 166.80 ppm, vinyl carbons at 135.74–125.83 ppm, methine carbon resonance (−$\underline{C}$H(CH_3)−O−CH_2) at 77.03−76.69, methylene carbon resonance (−$\underline{C}H_2$ −O−CH<) at 73.98−73.72, methylene carbon of the methacrylate group ($\underline{C}H_2$–O–C(=O)) around 64.99−64.78 and methyl groups as multiplet at 19.12–17.41 ppm. The methylene carbons connected with phosphate ester group OP–O–$\underline{C}H_2$ are observed in the region 72.58–71.86 ppm, and the methine carbon connected with phosphate ester group OP–O–$\underline{C}$H appears at 71.15 ppm.

^{31}P NMR spectrum exhibits a multiplet around −3.18 ppm attributed to the phosphate ester group of HFPOEM-2. The above results demonstrate the successful synthesis of HFPOEM-2, which is excellent agreement with FTIR analysis. The data presented above verify the successful synthesis of HFPOEM-3, showing a high degree of consistency with the FTIR spectroscopic data.

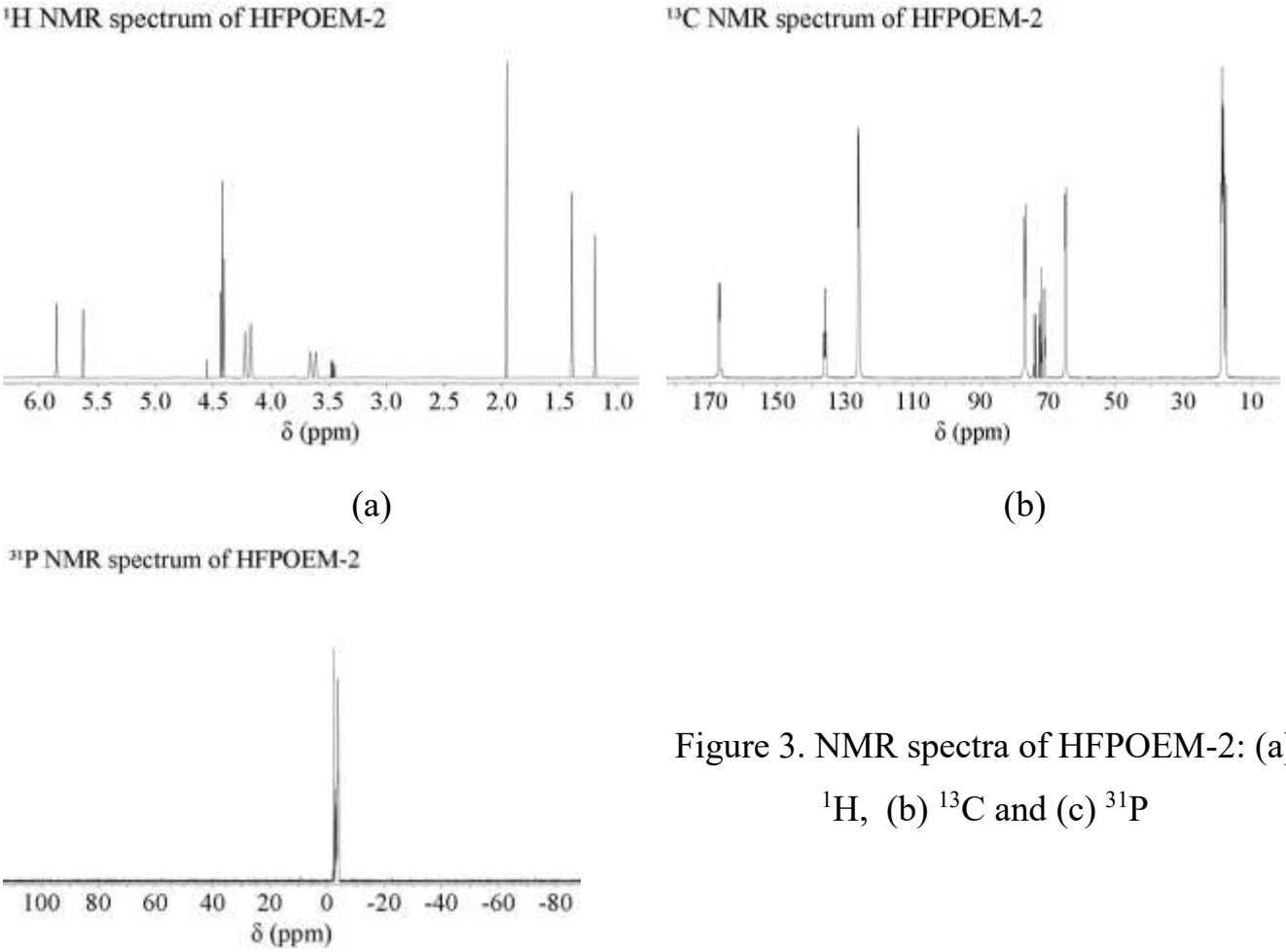


Figure 3. NMR spectra of HFPOEM-2: (a) ^{1}H, (b) ^{13}C and (c) ^{31}P

The ^{1}HNMR spectrum of HFPOEM-3 is shown in Figure 4-a. Aromatic resonances (–CH=C<u>H</u>– and –C<u>H</u>=CH–) are observed at δ 7.14–6.83 ppm, while characteristic methacrylate vinyl signals (=C<u>H</u>$_2$) appear at δ 5.84–5.61 ppm, indicating preserved polymerizable double bonds. Methylene protons of methacrylate (C(=O)–O–C<u>H</u>$_2$) resonate as multiplet around δ= 4.41 ppm, and the protons of methylene connected to phosphate ester group are observed as multiplet around δ= 4.24 ppm. Additionally, the methyl group of methacrylate appears at δ 1.93 ppm; correspondingly, the methyl group of aromatic spacer is detected around δ 1.59 ppm.

^{13}C NMR spectrum of HFPOEM-3 further supports the proposed chemical structure illustrated in Figure 4-b, showing ester carbonyl carbons (O–<u>C</u>=O) at δ 174.27 ppm, aromatic/vinyl carbons (=<u>C</u>< and =<u>C</u>H–) at around 165.74, 149.56,

141.55, 133.42 and 119.69 ppm, vinyl carbon of methacrylate (>C=$\underline{C}H_2$) around 131.09 ppm, methylene carbon of methacrylate (CO)O–$\underline{C}H_2$) at 68.89 ppm, methylene carbon of ester (OP–O–$\underline{C}H_2$) around 66.93 ppm, quaternary carbon (>C<) at 42.98 and methyl groups ($\underline{C}H_{3group}$) at 31.05 and 18.02 ppm.

In the ^{31}P NMR spectrum of HFPOEM-3, there is only single sharp resonance at δ= −2.83 ppm, which matches well with proposed chemical structure of HFPOEM-3.

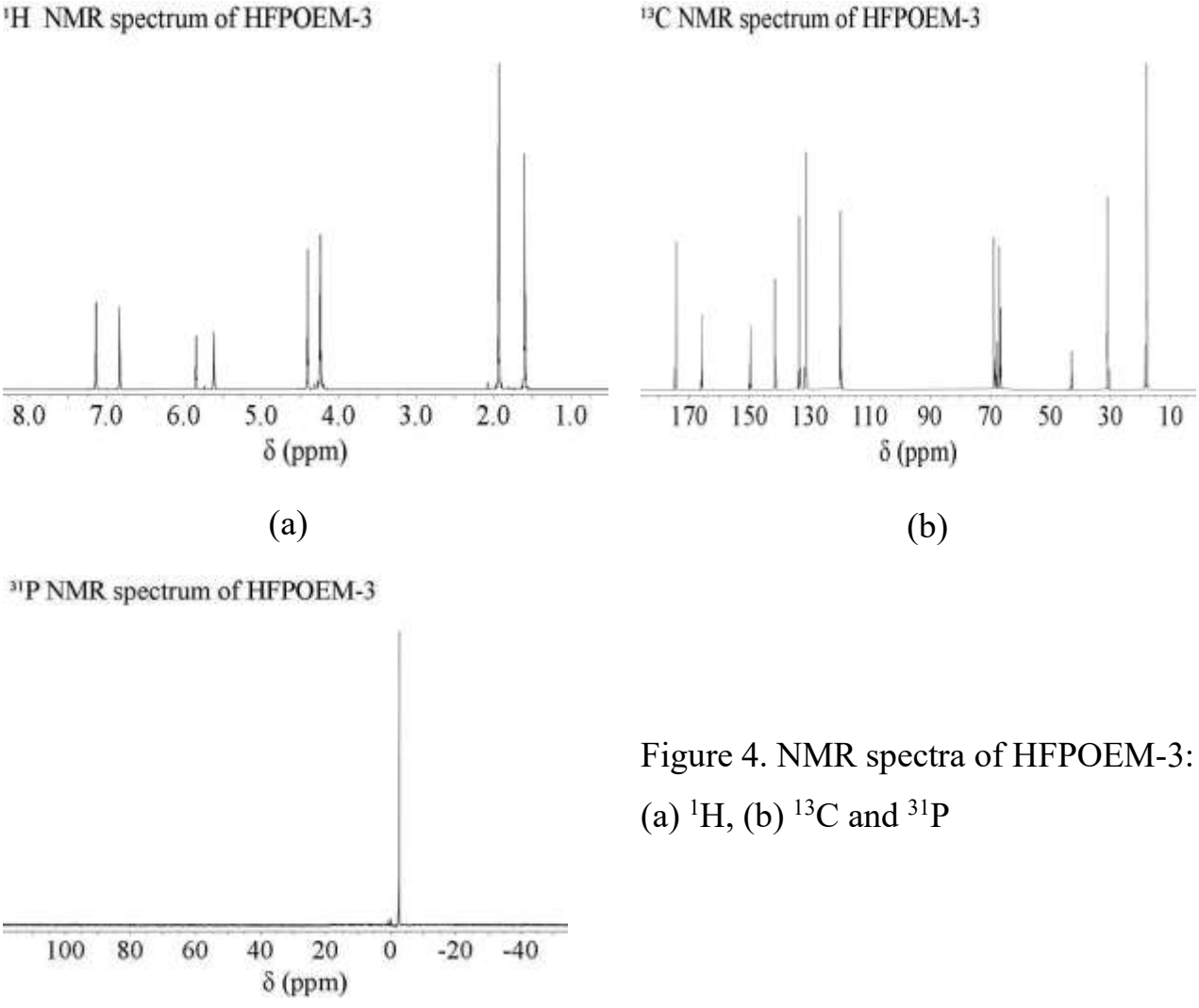


Figure 4. NMR spectra of HFPOEM-3: (a) ^{1}H, (b) ^{13}C and ^{31}P

3.2. Effect of spacers on thermal curing behaviour

Non-isothermal curing kinetics of HFPOEM-1, HFPOEM-2, and HFPOEM-3 were investigated via DSC at a constant heating rate of 10 °C/min, employing BPO as

the free-radical initiator. The resulting thermograms exhibited well-defined, single exothermic peaks (Figure 5) for all samples, corresponding to the polymerization and crosslinking reactions. The thermal transition parameters, including the onset temperature of exothermic peak (T_{ons}), maximum temperature of exothermic peak (T_p), endset temperature of exothermic peak (T_{end}), and total enthalpy of reaction (ΔH_{tot}), were determined from the DSC profiles (Table 1) to study the curing kinetics of the HFPOEM samples and to evaluate the influence of the spacers on the polymerization processes.

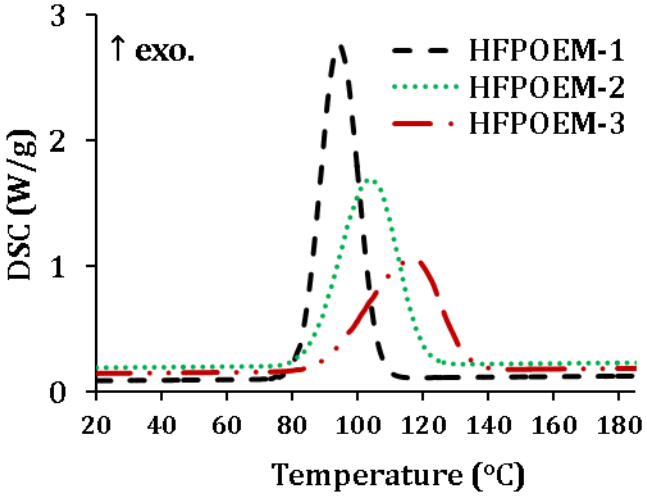


Figure 5. DSC curves of HFPOEM samples

Table 1. Thermal parameters from DSC curves

Samples	T_{ons} (°C)	T_p (°C)	T_{end} (°C)	ΔH_{tot} (J/g)
HFPOEM-1	81	95	108	221.7
HFPOEM-2	84	104	120	185.5
HFPOEM-3	96	118	133	119.2

As shown in Table 1 for HFPOEM-1, the exothermic reaction begins at T_{ons}= 81 °C, reaches its maximum at T_p= 95 °C, and ends at T_{end}= 108 °C, releasing a total enthalpy of ΔH_{tot} = 221.7 J/g. The relatively low onset temperature suggests that the reactive sites within HFPOEM-1 are activated at comparatively low thermal energy. In addition, the high enthalpy value indicates that a significant amount of heat is released during the reaction, implying a higher extent of chemical transformation or cross-link formation within the material. In comparison, HFPOEM-2 exhibits an exothermic event that starts at T_{ons}= 84 °C, reaches its maximum at T_p = 104 °C, and terminates at T_{end} = 120 °C, with a total heat release of ΔH_{tot}= 185.5 J/g. The shift of the peak temperature toward higher values relative to HFPOEM-1 indicates that a higher thermal activation energy is required

to initiate the reaction, suggesting a moderate increase in thermal stability. The slightly reduced enthalpy value compared with HFPOEM-1 may reflect a lower density of reactive sites or a reduced degree of cross-linking during the exothermic process. A more pronounced shift toward higher temperatures is observed for HFPOEM-3, where the reaction begins at T_{ons}= 96 °C, reaches its maximum at T_p= 118 °C, and concludes at T_{end}= 133 °C, with a significantly lower heat release of ΔH_{tot} = 119.2 J g^{-1}. The higher onset and peak temperatures indicate that HFPOEM-3 possesses the highest thermal stability among the three compounds, requiring greater thermal energy to activate the reaction. Furthermore, the lower enthalpy value indicates a reduced extent of the exothermic transformation, which may be attributed to the presence of structural rigidity or intermolecular steric hindrance within the molecular structure. Overall, the curing reactivity followed the sequence HFPOEM-1 > HFPOEM-2 > HFPOEM-3, confirming the critical role of the molecular structure and the spacer engineering in controlling polymerization behavior and thermal response.

3.3. Thermal degradation and flame-retardant performance of HFPOEMs

The thermogravimetric behavior of HFPOEM-1, HFPOEM-2, and HFPOEM-3 was evaluated at a heating rate of 10 °C min^{-1} in order to clarify the influence of spacer structure on the thermal stability and degradation characteristics of the materials. As shown in Figure 6, the main thermal decomposition of all samples occurs in a multistep manner within the temperature range of approximately 240–450 °C, which is characteristic of phosphate-containing polymeric systems. However, distinct differences in degradation behavior are observed as a function of spacer chemistry. Among the investigated materials, the aliphatic-spacer-containing HFPOEM-2 demonstrates slightly higher thermal stability than the spacer-free HFPOEM-1. As shown in Figure 6 and Table 2, HFPOEM-2 displays a higher temperatures at 5%, 10%, and 50% weight loss (T_5% = 265 °C, T_{10}%= 276 °C, and T_{50}%= 362 °C) compared to HFPOEM-1 (T_5% = 258 °C T_{10}%= 268 °C, and T_{50}%= 357 °C), indicating enhanced resistance to thermal degradation in the

presence of the aliphatic spacer. This behavior can be primarily attributed to the higher functionality of the HFPOEM-2 monomer (functionality = 4, compared to 3 for HFPOEM-1), arising from the presence of four methacrylate groups. This increased functionality promotes the formation of a more densely crosslinked polymer network, thereby increasing the effective crosslink density and improving thermal stability.

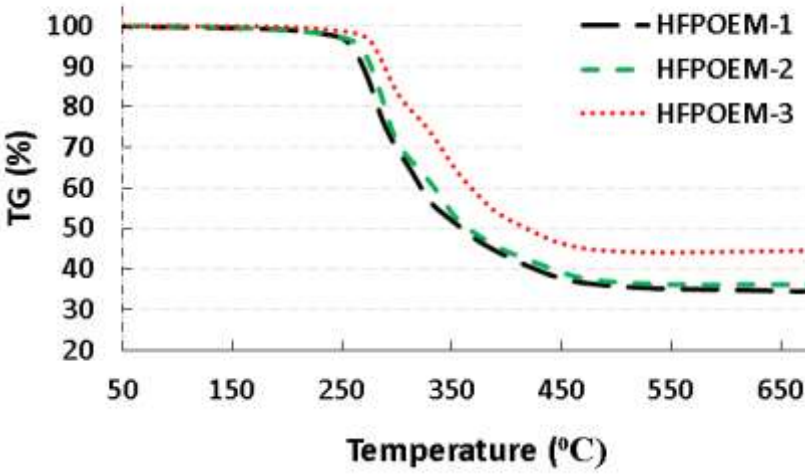


Figure 6. TGA curves of cured samples

The presence of the aromatic-spacer-containing HFPOEM-3 exhibits the highest thermal stability, with the entire degradation profile shifted toward higher temperatures The data presented in Figure 6 and Table 2 show that HFPOEM-3 reaches temperatures at 5%, 10%, and 50% weight loss of approximately 279 °C, 289 °C, and 418 °C, respectively. The superior thermal performance of HFPOEM-3 can be attributed to the presence of the rigid aromatic spacer, which increases chain stiffness and restricts segmental mobility, thereby suppressing early bond scission during heating. Upon thermal activation, the cleavage of phosphate ester linkages leads to the formation of phosphorus-containing acidic species, which promote dehydration and crosslinking reactions in the condensed phase. In the case of HFPOEM-3, the aromatic spacer further facilitates aromatization and carbonization processes, resulting in the formation of a thermally stable carbonaceous structure that effectively retards mass loss at elevated temperatures.

At higher temperatures, the percent of char yield at 600°C follows the order HFPOEM-3 > HFPOEM-2 > HFPOEM-1, as clearly observed in Figure 6 and Table 2 . HFPOEM-3 exhibits the highest char yield, approximately ≈ 44%, reflecting its enhanced condensed-phase stabilization and carbonization efficiency. In contrast, HFPOEM-2 and HFPOEM-1 show lower char residues, around ≈ 36%, with HFPOEM-2 retaining slightly more char than HFPOEM-1.

Table 2 Thermal decomposition temperatures and residue at 600˚C

Sample	$T_{5\%}$ (°C)	$T_{10\%}$ (°C)	T_{max} (°C)	Residue at 600 °C (wt %)
HFPOEM -1	258	268	357	34.9
HFPOEM -2	265	276	362	36.1
HFPOEM -3	279	289	418	44.3

Regarding the fire-retardant efficacy, the limiting oxygen index (LOI) values followed a different trend: HFPOEM-1 (31.6) > HFPOEM-2 (30.5) > HFPOEM-3 (29.7), as summarized in Table 3. The data obtained indicate that the samples containing spacers have slightly lower LOI values compared to the sample without spacer. This behavior is fundamentally governed by an interdependent relationship between the phosphorus content and the spacer structure. Notably, although the aliphatic-spacer system (HFPOEM-2) possessed the highest phosphorus content (7.74 wt%), its LOI slightly decreased, suggesting that the inherent flammability of the aliphatic fragments partially counteracts the flame-retardant contribution of the phosphorus. Conversely, the aromatic-spacer system (HFPOEM-3) exhibited the lowest LOI, directly reflecting its lower phosphorus loading (6.7 wt%). The results obtained summarize that while phosphorus content remains the primary determinant of fire resistance, the chemical structure of the spacer plays a pivotal role in modifying the overall flame-retardant performance..

Table 3 limiting oxygen index (LOI) and gel-fraction

Sample	Gel-fraction of curing samples (%)	P (wt %)	LOI (%)
HFPOEM -1	99.1	7.14	31.6
HFPOEM -2	98.5	7.74	30.5
HFPOEM **-3**	97.8	6.70	29.7

To evaluate the degree of crosslinking within HFPOEM matrices (thermally cured using 0.5 wt% peroxide), gel fraction measurements were conducted via soxhlet extraction using toluene as the solvent. As summarized in Table 4, all systems exhibit high gel fractions exceeding 96%, indicating the formation of highly crosslinked polymer networks. These results suggest that the incorporation of spacer units within the HFPOEM structures does not significantly hinder the conversion of methacrylate fragments into three-dimensional crosslinked network.

3.4. Effect of Spacers on Physical-Mechanical Properties of HFPOEMs

Practically, achieving a balanced combination of flame retardancy and mechanical performance remains a significant challenge in polymer systems, wherein improvements in fire resistance are often accompanied by a reduction in mechanical properties. Therefore, the effects of incorporating aliphatic and aromatic spacers on the mechanical properties, such as tensile strength, elongation at break and modulus, have been systematically examined. The stress–strain curves of the HFPOEM systems, as illustrated in Figure 7, notably demonstrate a significant dependence of the mechanical performance on the presence of the spacer and its chemical structure. The results in Table 4 indicate that the sample without a spacer (HFPOEM-1) exhibits the poorest mechanical performance, characterized by the lowest tensile strength and deformability at break, reaching a maximum stress (σ_{max}) of 17.5 MPa at a relatively low elongation at break (ε_{break}) of 1.5%. This may be because the absence of soft (flexible) and hard (rigid) segments hinder stress redistribution under tensile loading, resulting in early

fracture after the elastic deformation regime. In other words, the incorporation of flexible and rigid fragments is beneficial for tensile stress resistance in OEAs.

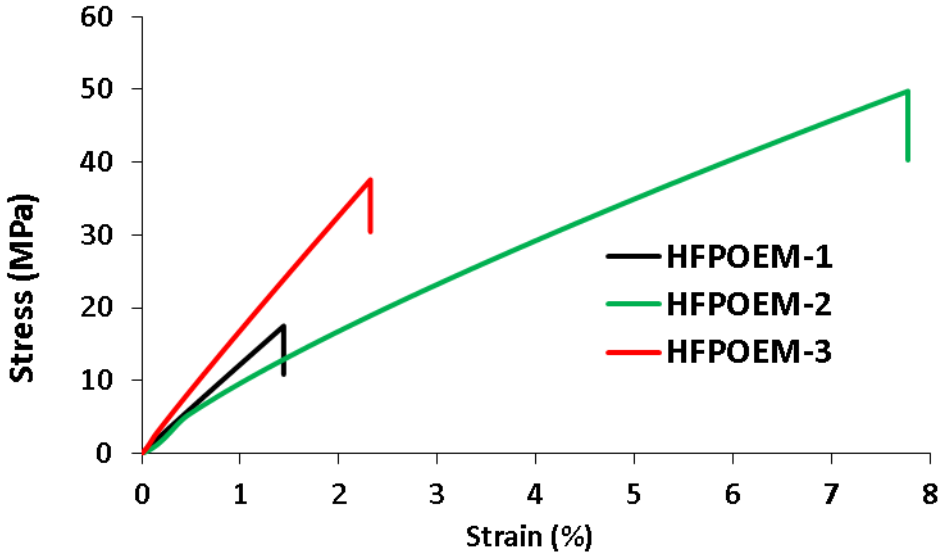


Figure 7 Stress–strain curves of HFPOEM cured samples

Remarkably, from Figure 7 and table 4, it is evident that the incorporation of flexible spacer (TPG) into the backbone of HFPOEM-2 polymer shows highest enhancement in elongation at break (7.8%) and tensile strength (49.9 MPa), due to the effects that the orientation of its network chain containing the soft group has on the fracture process. The presence of flexible aliphatic spacer increases segmental mobility and facilitates more efficient dissipation of applied stress along the polymer chains, thereby delaying crack initiation and propagation. Furthermore, the integration of rigid spacer into the HFPOEM-3 backbone can also promotes production of a polymer characterized by elevated values of elongation at break, and tensile strength reaching 2.3%, and 37.6 MPa, respectively, relative to the spacer-free polymer (HFPOEM-1). The rigid aromatic spacer enhances load transfer efficiency and increases the stiffness of the polymer network, which accounts for the higher σ_{max} relative to HFPOEM-1. However, restricted rotation of aromatic structure limits chain extensibility, resulting in lower ductility compared to HFPOEM-2. These results clearly demonstrate that the

introduction of a flexible aliphatic spacer is most effective for simultaneously enhancing strength and ductility, whereas the aromatic spacer primarily improves strength through increased rigidity at the expense of extensibility. The spacer-free structure, by comparison, remains relatively brittle due to limited chain mobility.

Table 4 Physical-Mechanical Properties of HFPOEMs

Sample	Tensile strength, (MPa)	Elongation at break, dl (%)
HFPOEM -1	17.5	1.5
HFPOEM -2	49.9	7.8
HFPOEM -3	37.6	2.3

4. Conclusion

In this study, a series of halogen-free phosphate-containing oligoester methacrylates (HFPOEMs) with systematically varied spacer structures were successfully synthesized and evaluated. The curing behavior revealed a progressive decrease in reactivity upon spacer incorporation, with the peak curing temperature shifting from 95 °C for the spacer-free system (HFPOEM-1) to 104 °C and 118 °C for the aliphatic-spacer system (HFPOEM-2) and aromatic-spacer system (HFPOEM-3) systems, respectively, accompanied by a reduction in total reaction enthalpy from 221.7 to 119.2 J/g. This trend reflects increased steric hindrance and reduced accessibility of reactive groups in spacer-containing systems.

Mechanical performance was markedly enhanced by spacer engineering. The aliphatic spacer system (HFPOEM-2) exhibited the highest tensile strength (49.9 MPa) and elongation at break (7.8%), representing nearly a threefold increase in strength and over fivefold improvement in ductility compared to the spacer-free system (17.5 MPa and 1.5%). In contrast, the aromatic spacer system (HFPOEM-3) showed intermediate mechanical performance (37.6 MPa, 2.3%), indicating improved stiffness but limited

extensibility due to restricted chain mobility. The flame-retardant performance showed only slight variation, with LOI values between 29.7% and 31.6%. In summary, spacer modification is an effective approach to adjust the balance between mechanical properties and thermal stability. The aliphatic spacer improves toughness, while the aromatic spacer enhances thermal resistance, providing promising directions for designing halogen-free flame-retardant polymer systems.

Funding declaration: The authors received no financial support for the research, authorship, and/or publication of this article.

Conflict of interest statement

No potential conflict of interest was reported by the authors.

References

[1] X. Yin, L. Li, H. Pang, Y. Luo, and B. Zhang, "Halogen-free instinct flame-retardant waterborne polyurethanes: composition, performance, and application," 2022. doi: 10.1039/d2ra01822e.

[2] L. Wan *et al.*, "Flame-retarded thermoplastic polyurethane elastomer: From organic materials to nanocomposites and new prospects," *Chem. Eng. J.*, vol. 417, p. 129314, Aug. 2021, doi: 10.1016/j.cej.2021.129314.

[3] A. K. J. Al-Hamzawi, B. A. Buravov, S. M. Solomakhin, L. Y. Donetskova, O. O. I. Tuzhikov, and O. O. I. Tuzhikov, "Synthesis of new phosphorus-containing oligoester methacrylates by using aliphatic and aromatic spacers," *J. Polym. Res.*, vol. 32, no. 6, p. 195, Jun. 2025, doi: 10.1007/s10965-025-04388-y.

[4] M. Rakotomalala, S. Wagner, and M. Döring, "Recent Developments in Halogen Free Flame Retardants for Epoxy Resins for Electrical and Electronic Applications," *Materials (Basel).*, vol. 3, no. 8, pp. 4300–4327, Aug. 2010, doi: 10.3390/ma3084300.

[5] S.-H. Chiu, C.-L. Wu, H.-T. Lee, J.-H. Gu, and M.-C. Suen, "Synthesis and characterisation of novel flame retardant polyurethanes containing designed phosphorus units," *J. Polym. Res.*, vol. 23, no. 10, p. 205, Oct. 2016, doi: 10.1007/s10965-016-1098-y.

[6] S. V. Borisov *et al.*, "Low Flammability Polymers Based on Phosphorus-Containing Methacrylates," *Polym. Sci. - Ser. B*, vol. 66, no. 2, pp. 269–278, Apr. 2024, doi: 10.1134/S1560090424600426.

[7] X. Chen and C. Jiao, "Thermal degradation characteristics of a novel flame retardant coating using TG-IR technique," *Polym. Degrad. Stab.*, vol. 93, no. 12, pp. 2222–2225, Dec. 2008, doi: 10.1016/j.polymdegradstab.2008.09.005.

[8] H. Liang and W. Shi, "Thermal behaviour and degradation mechanism of

phosphate di/triacrylate used for UV curable flame-retardant coatings," *Polym. Degrad. Stab.*, vol. 84, no. 3, pp. 525–532, Jun. 2004, doi: 10.1016/j.polymdegradstab.2003.11.006.

[9] J.-A. Choi, Y. Kang, H. Shim, D. W. Kim, H.-K. Song, and D.-W. Kim, "Effect of the cross-linking agent on cycling performances of lithium-ion polymer cells assembled by in situ chemical cross-linking with tris(2-(acryloyloxy)ethyl) phosphate," *J. Power Sources*, vol. 189, no. 1, pp. 809–813, Apr. 2009, doi: 10.1016/j.jpowsour.2008.07.048.

[10] G. Ilia, L. Macarie, N. Plesu, S. Iliescu, and A. Popa, "Solvent-free synthesis of tris(4-hydroxybutyl acrylate) phosphate in the presence of 1-methylimidazole," *J. Iran. Chem. Soc.*, vol. 15, no. 1, pp. 17–21, Jan. 2018, doi: 10.1007/s13738-017-1204-z.

[11] Y. Li *et al.*, "A bio-derived char-forming strategy for surface fireproofing: Functionalization of UV-curing flame-retardant coating with vinyl-modified tannic acid," *Eur. Polym. J.*, vol. 148, p. 110358, Apr. 2021, doi: 10.1016/j.eurpolymj.2021.110358.

[12] C. Yao, W. Xing, C. Ma, L. Song, Y. Hu, and Z. Zhuang, "Synthesis of phytic acid-based monomer for UV-Cured coating to improve fire safety of PMMA," *Prog. Org. Coatings*, vol. 140, p. 105497, Mar. 2020, doi: 10.1016/j.porgcoat.2019.105497.

[13] C. Luo, J. Zuo, F. Wang, Y. Yuan, F. Lin, and J. Zhao, "Preparation and Properties of Halogen-Free Flame Retardant and High Refractive Index Optical Resin via Click Chemistry," *Macromol. Res.*, vol. 26, no. 4, pp. 346–352, Apr. 2018, doi: 10.1007/s13233-018-6045-8.

[14] M. S. Özer and S. Gaan, "Recent developments in phosphorus based flame retardant coatings for textiles: Synthesis, applications and performance," *Prog. Org. Coatings*, vol. 171, p. 107027, Oct. 2022, doi: 10.1016/j.porgcoat.2022.107027.

[15] P. Joseph, M. Arun, S. Bigger, M. Guerrieri, D. Pospiech, and C. Harnisch, "Mode of Action of Condensed- and Gaseous-Phase Fire Retardation in Some Phosphorus-Modified Polymethyl Methacrylate- and Polystyrene-Based Bulk Polymers," *Polymers (Basel).*, vol. 13, no. 19, p. 3402, Oct. 2021, doi: 10.3390/polym13193402.

[16] P. Li, J. Wang, C. Wang, C. Xu, and A. Ni, "The Flame Retardant and Mechanical Properties of the Epoxy Modified by an Efficient DOPO-Based Flame Retardant," *Polymers (Basel).*, vol. 16, no. 5, p. 631, Feb. 2024, doi: 10.3390/polym16050631.

[17] S. V. Levchik, “Introduction to Flame Retardancy and Polymer Flammability,” in *Flame Retardant Polymer Nanocomposites*, Wiley, 2007, pp. 1–29. doi: 10.1002/9780470109038.ch1.

[18] E. Rezvani Ghomi *et al.*, “The Flame Retardancy of Polyethylene Composites: From Fundamental Concepts to Nanocomposites,” *Molecules*, vol. 25, no. 21, p. 5157, Nov. 2020, doi: 10.3390/molecules25215157.

[19] B. Schartel, “Phosphorus-based Flame Retardancy Mechanisms—Old Hat or a Starting Point for Future Development?,” *Materials (Basel).*, vol. 3, no. 10, pp. 4710–4745, Sep. 2010, doi: 10.3390/ma3104710.

[20] A. R. Horrocks, P. J. Davies, B. K. Kandola, and A. Alderson, “The Potential for Volatile Phosphorus-containing Flame Retardants in Textile Back-coatings,” *J. Fire Sci.*, vol. 25, no. 6, pp. 523–540, Nov. 2007, doi: 10.1177/0734904107083553.

[21] N. Bouvet, G. T. Linteris, V. I. Babushok, F. Takahashi, V. R. Katta, and R. Krämer, “A comparison of the gas-phase fire retardant action of DMMP and Br2 in co-flow diffusion flame extinguishment,” *Combust. Flame*, vol. 169, pp. 340–348, Jul. 2016, doi: 10.1016/j.combustflame.2016.04.023.

[22] D. Hao, X. Guo, X. Zhu, C. Wei, L. Gao, and X. Wang, “Progress in synthesis, modification, characterization and applications of hyperbranched polyphosphate polyesters,” *Des. Monomers Polym.*, vol. 27, no. 1, pp. 62–86, Dec. 2024, doi: 10.1080/15685551.2024.2376842.

[23] F. Bier, J. Six, and A. Durand, “DOPO-Based Phosphorus-Containing Methacrylic (Co)Polymers: Glass Transition Temperature Investigation,” *Macromol. Mater. Eng.*, vol. 304, no. 4, Apr. 2019, doi: 10.1002/mame.201800645.

[24] V. P. Feitosa *et al.*, “The role of spacer carbon chain in acidic functional monomers on the physicochemical properties of self-etch dental adhesives,” *J. Dent.*, vol. 42, no. 5, pp. 565–574, May 2014, doi: 10.1016/j.jdent.2014.02.009.

[25] Z. Wang and B. Liang, “Synthesis and properties of phosphorus and nitrogen containing intumescent flame-retardant curing agent for epoxy resin,” *Plast. Rubber Compos.*, vol. 47, no. 7, pp. 306–314, Aug. 2018, doi: 10.1080/14658011.2018.1491702.

[26] I. E. Nifant'ev and P. V. Ivchenko, "Design, Synthesis and Actual Applications of the Polymers Containing Acidic P–OH Fragments: Part 1. Polyphosphodiesters," *Int. J. Mol. Sci.*, vol. 23, no. 23, p. 14857, Nov. 2022, doi: 10.3390/ijms232314857.

[27] X.-F. Liu *et al.*, "A novel phosphorus-containing semi-aromatic polyester toward flame retardancy and enhanced mechanical properties of epoxy resin," *Chem. Eng. J.*, vol. 380, p. 122471, Jan. 2020, doi: 10.1016/j.cej.2019.122471.

[28] Z. Lin, Y. Cong, B. Zhang, and H. Huang, "Synthesis and characterisation of a novel Y-shaped liquid crystalline epoxy and its effect on isotropic epoxy resin," *Liq. Cryst.*, vol. 46, no. 10, pp. 1467–1477, Aug. 2019, doi: 10.1080/02678292.2018.1545935.

[29] O. O. Tuzhikov *et al.*, "Rheological properties of phosphorus-containing oligoester(meth)acrylate for processing by vacuum infusion," *Fine Chem. Technol.*, vol. 19, no. 5, pp. 441–451, Nov. 2024, doi: 10.32362/2410-6593-2024-19-5-441-451.

[30] B. A. Buravov, E. S. Bochkarev, A. Al-Khamzawi, N. V. Sidorenko, O. O. Tuzhikov, and O. I. Tuzhikov, "STUDY OF THE INFLUENCE OF SPACER ON FEATURES OF UV CURING OF PHOSPHOROSE-CONTAINING METACRYLATES OF VARIOUS FUNCTIONALITY," *Izv. Volgogr. STATE Tech. Univ.*, no. 12(247), pp. 136–143, Dec. 2020, doi: 10.35211/1990-5297-2020-12-247-136-143.

[31] B. A. Buravov *et al.*, "Synthesis of new photo-cured phosphorus-containing oligoestermethacrylates with a spacer in the structure," *Fine Chem. Technol.*, vol. 17, no. 5, pp. 410–426, Nov. 2022, doi: 10.32362/2410-6593-2022-17-5-410-426.

[32] B. A. Buravov, E. S. Bochkarev, A. Al-Khamzawi, O. O. Tuzhikov, and O. I. Tuzhikov, "MODERN TRENDS IN THE DEVELOPMENT OF ANTIPYRENE FOR POLYMER COMPOSITIONS. COMPOSITION, PROPERTIES, APPLICATION," *Izv. Volgogr. STATE Tech. Univ.*, no. 12(247), pp. 7–24, Dec. 2020, doi: 10.35211/1990-5297-2020-12-247-7-24.

[33] B. A. Buravov *et al.*, "Influence of the structure of phosphorus(III)-containing oligoester(meth)acrylates on the physical and mechanical properties, thermal stability, and combustion mechanisms of cured polymers," *Fine Chem. Technol.*, vol. 20, no. 6, pp. 594–611, Jan. 2026, doi: 10.32362/2410-6593-2025-20-6-594-611.

[34] S. L. Barbot'ko *et al.*, "Reinforced composite materials based on phosphorus-containing binders with promising physical, mechanical and fireproof properties," *Him. Fiz. i mezoskopiâ*, vol. 26, no. 1, pp. 69–84, 2024, doi: 10.62669/17270227.2024.1.7.

[35] X. Chen, C. Jiao, S. Li, and J. Sun, "Flame retardant epoxy resins from bisphenol-A epoxy cured with hyperbranched polyphosphate ester," *J. Polym. Res.*, vol. 18, no. 6, pp. 2229–2237, Nov. 2011, doi: 10.1007/s10965-011-9636-0.

[36] X. Huang, X. Zhao, M. Zhang, Y. Xu, H. Zhi, and J. Yang, "Green Synthesis of Triaryl Phosphates with POCl 3 in Water," *ChemistrySelect*, vol. 2, no. 34, pp. 11007–11011, Dec. 2017, doi: 10.1002/slct.201702215.

[37] Q. Wang and W. Shi, "Synthesis and thermal decomposition of a novel hyperbranched polyphosphate ester used for flame retardant systems," *Polym. Degrad. Stab.*, vol. 91, no. 6, pp. 1289–1294, Jun. 2006, doi: 10.1016/j.polymdegradstab.2005.09.001.